NASA TECHNICAL NOTE

NASA TN D-4841

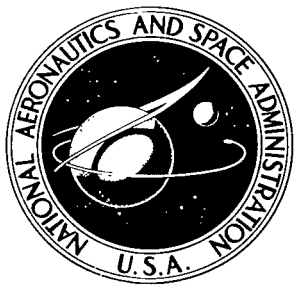

NASA TN D-4841

USE OF AN ELECTROLUMINESCENT DISPLAY IN MANUAL TRACKING AND IN A READING TASK

by Frank Neuman and John D. Foster

Ames Research Center
Moffett Field, Calif.

NATIONAL AERONAUTICS AND SPACE ADMINISTRATION • WASHINGTON, D. C. • OCTOBER 1968

USE OF AN ELECTROLUMINESCENT DISPLAY IN MANUAL TRACKING AND IN A READING TASK

By Frank Neuman and John D. Foster

Ames Research Center
Moffett Field, Calif.

NATIONAL AERONAUTICS AND SPACE ADMINISTRATION

For sale by the Clearinghouse for Federal Scientific and Technical Information
Springfield, Virginia 22151 – CFSTI price $3.00

USE OF AN ELECTROLUMINESCENT DISPLAY IN MANUAL TRACKING AND IN A READING TASK

By Frank Neuman and John D. Foster

Ames Research Center

SUMMARY

The purpose of this research was to determine whether performance differences existed between electromechanical and electroluminescent (EL) displays in a closed loop manual tracking task and in reading accuracy tests. Both displays had vertical scales, which are considered acceptable for spacecraft use.

Studies were made with two EL displays, a single-scale, and a double-scale bargraph display. Pursuit tracking of sine and random waves and readability tests were conducted. The double-scale instrument was used in the tracking tasks and the single-scale instrument in the readability tests. The discreteness of the EL instrument's 128 vertical scale segments (12.6/cm) did not appear to cause any problems in either task. In the tracking tasks, the electroluminescent instruments were comparable to the electromechanical instruments in the region of their flat frequency response. In the readability tests, in which the environmental illumination was changed, readability of the EL instruments reduced rapidly with increasing environmental illumination above 550 lumens/m^2. However, at the low ambient light conditions expected in a spacecraft environment, less than 1 lumen/m^2, the readability was adequate.

INTRODUCTION

Electroluminescent (EL) displays have certain advantages for aerospace applications. They can be controlled directly by a digital computer without the need of a digital to analog interface. They work at electronic speeds, a few orders of magnitude faster than electromechanical instruments, and allow variable scaling and quick changes in the data presented. However, they produce a relatively low level of emitted light intensity, and present continuous analog data in a sampled fashion by a column of discrete segments.

In this research effort, the displays were evaluated by comparing operator performance in three dynamic tasks. The displays used were two vertical scale EL instruments and an electromechanical instrument which had similar vertical scales. The EL instruments were developed for Ames Research Center under contract. They are described in detail in reference 1. The evaluation tasks chosen were relatively simple and no additional loading of the operator beyond the given task was provided. Two of the tasks, sine wave tracking and

random wave pursuit tracking, are widely reported on in the literature dealing with man-machine systems theory (see ref. 2 for a good summary). For the purpose of evaluation, a gross index of performance (standard deviation of the errors) was calculated for each instrument over a range of frequencies and bandwidths. Also, a refined scoring system for the random tracking task was developed and applied. The third task was a reading task designed to check instrument readability under varying environmental light conditions. The test consisted in reading values displayed for a short time interval on different instruments at different ambient light intensities. Calculations of rms errors were made under these conditions to evaluate the readability of the EL instrument as compared with the electromechanical instrument.

SYMBOLS

a	amplitude gain factor, average ratio of follow-up signal amplitude to command signal amplitude
$\varepsilon(t)$	$f_c(t) - f_f(t)$, total system error
$\varepsilon^*(t)$	error as modified by the display transfer functions
$\varepsilon_u(t)$	linearly uncorrelated error
$f_c(t)$	command signal
$f_f(f)$	system output
t_1	computer time delay
$t_2(f)$	instrument delay, function of frequency, time between input and output of corresponding amplitudes of a sine wave
$Y_c(s)$	transfer function of the controlled element
$Y_d(s)$	transfer function of the instrument
$Y_p(s)$	transfer operator representing the linear action of the subject
σ_j	standard deviation of the tracking error for the jth individual in a given test run
σ_p	root mean of the total system variances of the errors averaged over the individuals
σ_{u_j}	uncorrelated standard deviation of the error for the jth individual in a given test run

σ_{u_p} root mean of the uncorrelated system variances of the error averaged over the individuals

τ_d tracking delay, time shift required for maximum cross correlation between command and follow-up signal

DISPLAYS

In order to minimize the number of performance variables, the displays were chosen to have similar size and appearance.

Electroluminescent Displays

The electroluminescent displays are digitally controlled, designed for multipurpose display flexibility, and have bargraph formats to present digital information. Two EL displays were investigated in this report, a single- and a double-scale instrument.

Single-scale displays.- Figure 1 is a photograph of the single-scale instrument. The electronics of the instrument consist basically of a buffer, a register, and a decoder. The buffer accepts a 13-bit parallel word and an enable pulse from the computer. The enable pulse transfers the data into the

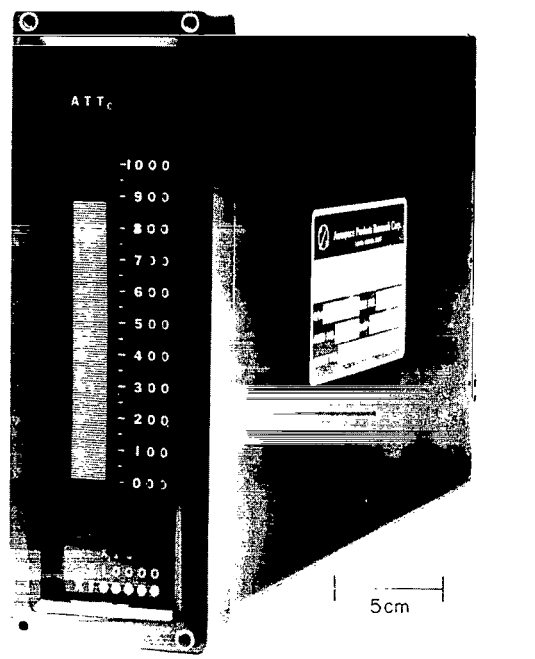

Figure 1.- Single scale EL instrument.

register. The data in the register is decoded to light the appropriate EL lamps. The instrument displays the data until it is readdressed or until the power is turned off. The length of time from the enable pulse until the proper lamps are turned on is 160 μsec. It requires 300 μsec to turn off the lamps. For this investigation, the frequency response of the instrument was limited only by the cycle time of the computer program (0.01 sec).

The shapes, actual sizes, and arrangement of the EL lamps are shown in figure 2(a). Lamps j, k, ℓ, and m specify the parameter displayed at a given time by illuminating an overlay scribed with the parameter name (see fig. 2(b)). The magnitudes of the data are represented in a bar format by turning on lamps a_1 through a_j where j can take on a value between 1 and 128. A multiplication factor, n, specifies which of the instrument scale lamps are to be turned on, lamp c for n = 1, lamps c and d for n = 10, and lamps c, d, and e for n = 100. The format can be changed to display a single segment only, a_j, by means of a switch. The EL lamp brightness is 13 ft-L. Lamps f, g, h, and i can serve to illuminate any desired data scribed into the display overlay.

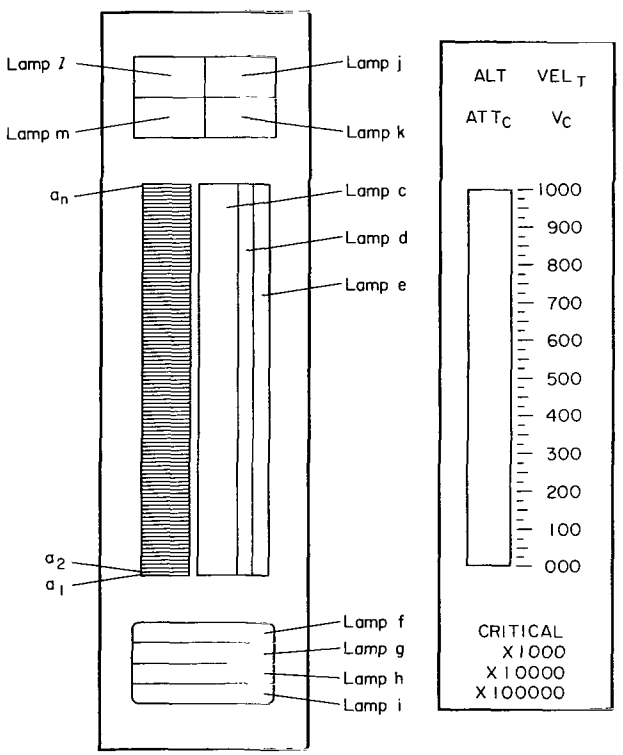

(a) EL lamp arrangement. (b) Display overlay.

Figure 2.- EL display details.

Double-scale display.- The double-scale EL instrument is essentially like the single-scale instrument with one additional vertical bar. However, since the instrument has only 13 data lines to the computer, two sequential words are needed. One word controls the same lamps described for the single-scale instrument. The other word controls the additional bar. Figure 3 is a photograph of the double-scale instrument. For the tracking task, the right scale was the command display, and the left scale was the follow-up display.

DC Meter Electromechanical Display

The electromechanical instrument was a galvanometer instrument with a light source and a spot reflected from a moving mirror as a readout (Fig. 4). Two of these instruments were placed side by side to allow for the pursuit tracking task. As with the EL display, the right instrument was the command display and the left instrument was the follow-up display. The meter was computer controlled through the digital-to-analog converters. It was found from the frequency response, in figure 5, that the instrument was linear and acted as a critically damped second-order low pass filter with a break frequency of 2.5 Hz.

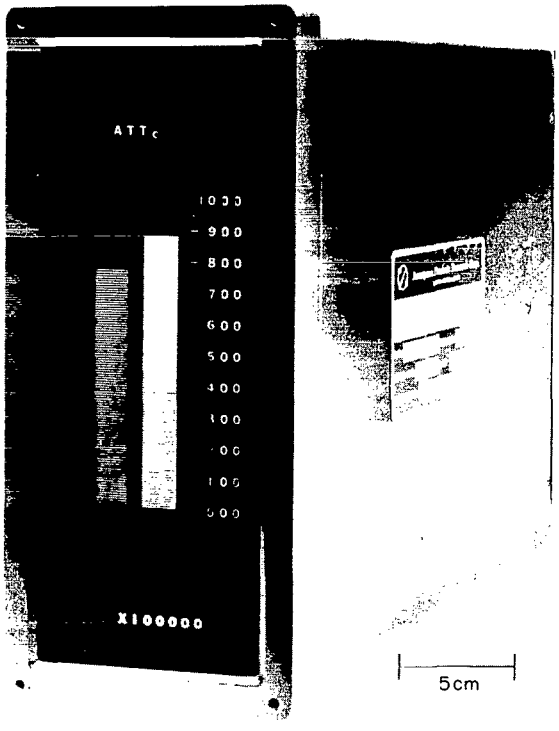

Figure 3.- Double scale EL instrument.

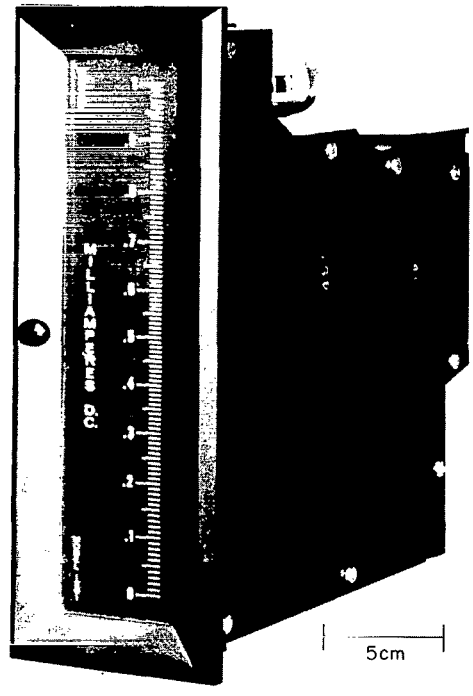

Figure 4.- DC meter instrument.

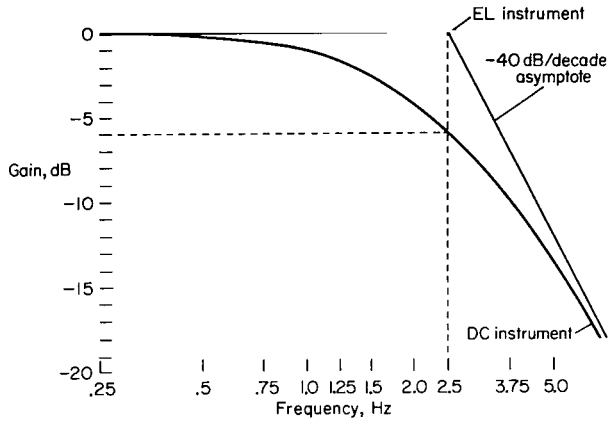

(a) Amplitude response.

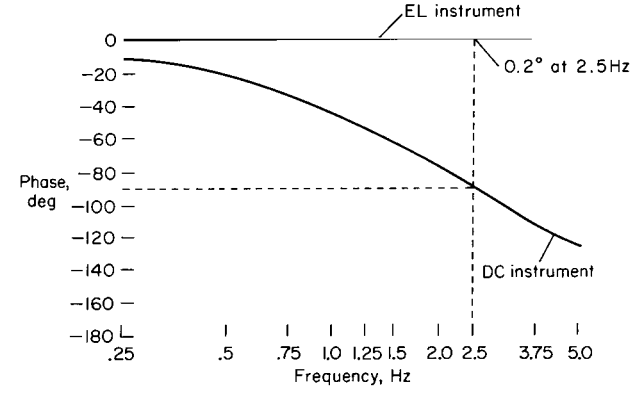

(b) Phase shift.

Figure 5.- Bode plot of amplitude and phase shift of the test instruments.

DESCRIPTION OF EXPERIMENTS

Tracking Tasks

Two types of pursuit tracking tasks were carried out: sine wave tracking and random wave tracking. For each task a function of time was displayed to the subject as motion of an indicator. The subject was required to track this function by moving a manual controller to position a second indicator. The object of the tracking task was to keep the indicators alined as closely as possible at all times.

The overall test setup is shown in figure 6. To track correctly, the subject would have to produce a follow-up signal which would lead the displayed command signal by a time $t_1 + t_2(f)$, where t_1 was the computer delay and $t_2(f)$ the instrument delay. The subjects could, at least in principle, make such a correction for the predictable sine wave tracking, but not for the random tracking.

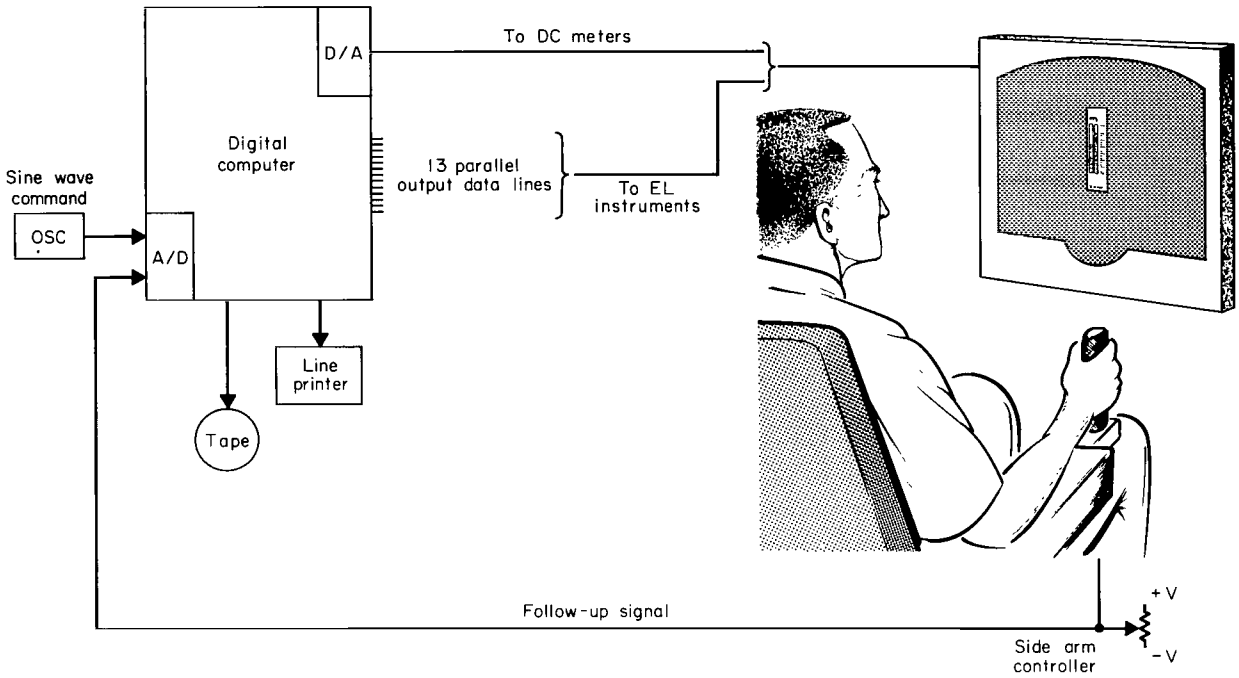

Figure 6.- Tracking task test setup.

A standard procedure was followed for each experiment. After experiment identification, data were displayed on the command display. The subject would then begin his tracking task. The computer would not begin to score his performance until the subject depressed a switch signalling the computer. This method excluded the errors associated with any starting transients. For each instrument, each of four subjects performed six sine wave tracking tasks in sequence with command frequencies and sampling rates as shown in table I.

TABLE I

Frequency, Hz	Sampling rate, samples/sec	Samples per experiment	Time per experiment, sec
0.1	100	30,000	300
.2	100	15,000	150
.4	100	7,500	75
.8	100	5,000	50
1.6	100	5,000	50
2.8	100	5,000	50

For the random tracking task, each of the four subjects tracked under six experimental conditions using each display. The bandwidths, sampling rates, and sample sizes of the random waveforms are shown in table II.

TABLE II

Bandwidth, Hz	Sampling rate, samples/sec	Samples per experiment	Time per experiment, sec
1/3	33.33	3000	90
1/3	33.33	9000	270
1/2	50	3000	60
1/2	50	9000	180
1	100	3000	30
1	100	9000	90

The command channel transmitted the signal that was to be tracked by the subject (see fig. 6). For the sine wave tracking task, the signal was generated by an oscillator, which was sampled periodically by the analog-to-digital converter (a/d). The computer scaled the data and converted them through a digital-to-analog converter to an appropriate DC signal to the DC instrument. To control the digital EL instrument command display the computer converted the data to a parallel digital word. For the random wave tracking task, the only difference was that the command function samples were stored in the computer before the session began, instead of being sampled during the session. These command function samples were generated off-line by the computer, as discussed in appendix A.

The subject sent the follow-up signal by means of the up and down motion (pitch axis) of a sidearm controller. The stick forces and displacement characteristics are shown in figure 7. The force gradient was chosen to be small to permit high-frequency tracking. The instruments were mounted on a display panel, which was painted black and had a replaceable center section. This arrangement allowed quick interchange of the different types of instruments.

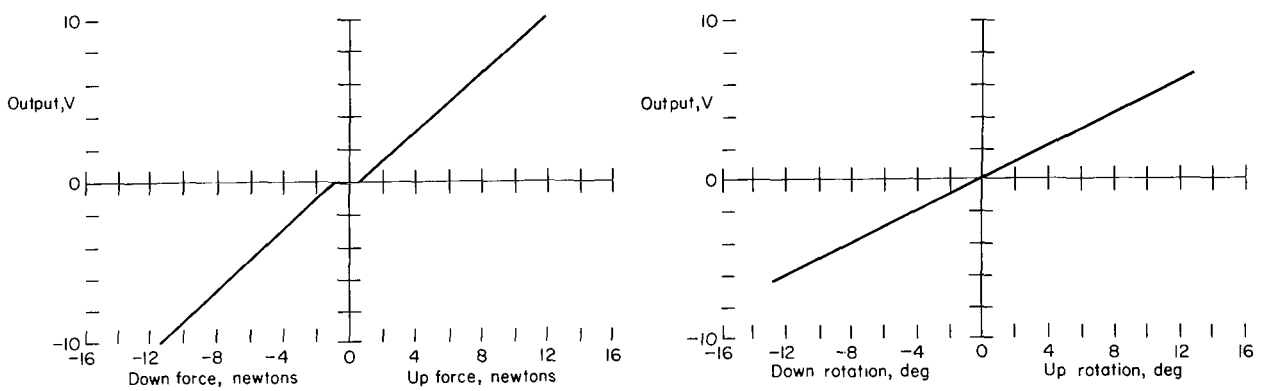

(a) Output vs. force.

(b) Output vs. displacement.

Figure 7.- Side-arm controller force and displacement curves.

The minimum sampling interval was 10 msec for the high-frequency tracking tasks. The time spent on data sampling, scaling, and output was only a small fraction of the sampling interval. These tasks completed, the computer stored the command value, calculated and stored the error, and generated an error histogram. Thus, the computer acted as a zero order hold circuit, which produced a delay of one-half of the sampling interval or 5 msec. This delay is equivalent to a 5° phase lag at 2.8 Hz, which is negligible compared to the other delays in the system, namely, human and instrument delays.

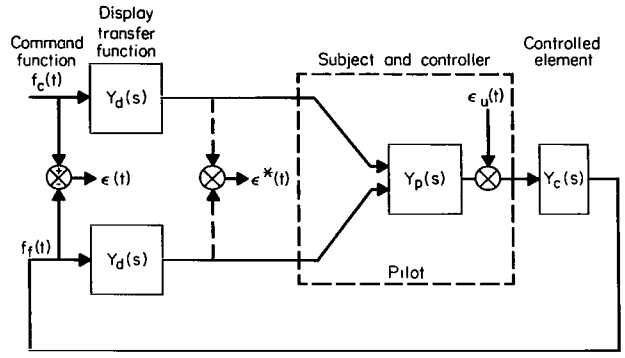

Figure 8.- Block diagram of pursuit tracking tasks.

The display in human tracking performance studies is normally a wideband linear oscilloscope, $Y_d(s) = k$, so that the difference in outputs, $\varepsilon^*(t)$, is always proportional to the system error, which is the difference between the command signal and the system output and depends primarily on $Y_p(s)$ and $Y_c(s)$. (See fig. 8.) The intent of this investigation was to study performance differences due to display limitations. The controlled element remained simple, $Y_c(s) = k$, while the displays with their transfer functions presented filtered versions of the command signal and systems output. The transfer functions were $Y_d(s) = k$ for the EL instrument, and $Y_d(s) = k/(s + a)^2$ for the DC instrument. Hence, in the present study, $\varepsilon^*(t)$ was primarily dependent on the performance of the particular display ($Y_d(s)$).

Display Readability Tests

To evaluate the readability of the EL display, a dynamic reading test was devised. The readability was tested as a function of the length of the data presentation time and of the illumination of the black instrument panel.

The subject started a test by pushing a button that signaled the computer to begin. The computer commanded a value for the display selected from a pseudo-random number generator. At the end of the desired display interval the computer returned the instrument value to zero and waited for the subject's reading to be entered. The subject orally indicated his reading to an assistant who typed it on the computer coupled typewriter. Following this, the computer calculated the reading error, incremented the error histogram, and displayed a new value on the instrument, which started the next cycle. For each instrument, each of four subjects performed 100 readings for each chosen time interval. These tests were repeated at three different instrument panel brightness levels.

The experimental setup for the readability tests differed slightly from the setup for the tracking tasks. The computer-instrument interface remained the same as the interface for the tracking tasks, except that the command

display was disconnected and only the follow-up display was controlled by the computer. The double scale EL display was replaced by the single-scale EL display, and only one DC meter was mounted on the display panel. In addition, six 500-W photo-spot lamps were suspended above and behind the subject's head to regulate the instrument panel glare. Each lamp was aimed to give a maximum reflected intensity at the center of the instrument. The reflected luminance was measured with a photometer with a 2° aperture aimed at the center of the instrument and placed at the subject's eye level. The illumination was calculated from the measured reflected luminance of a diffuse reflecting white surface.

The display interval (the length of time that a signal was applied to a given display) was determined by preliminary tests. Basic display intervals allowed the subject to barely read each display relatively easily without making gross errors. These intervals were 0.2 second for the EL instrument, and 0.35 second for the DC meter instrument. The intervals were too short for the DC instrument to reach steady state, and the subjects were instructed to read the maximum indicated values. For error computation purposes, these maximum values displayed on the DC meter were computed from the applied voltages, the transfer function of the instrument, and the time interval. It was determined theoretically, and confirmed by observation, that these maximum displayed values were always directly proportional to the steady-state input signal. The correction factor was 0.9. To increase the difficulty of the second test, the display intervals for the EL and DC meter were shortened by 0.1 second in order to generate statistically significant data. In this test, the maximum displayed values for the DC meter test were 0.84 of the steady-state value.

Off Line Data Reduction

Data were reduced during and after the individual tracking tests. The latter was done to get better insight into individual test results, and to obtain average performance parameters for the four individual subjects.

Graphical outputs were used to evaluate each tracking test. The graphical data included an amplitude versus time plot of the command function, $f_c(t)$, the follow-up function, $f_f(t)$, and the error function, $\varepsilon(t)$. As discussed in the section on results, the time delay (τ_d) and amplitude error (1-a) give a better insight into the performance than the standard deviation of error (σ_p). Therefore, these values were calculated for selected typical tests. In addition, the uncorrelated error functions $\varepsilon_u(t)$ and then σ_{u_p} were calculated.

To average over the test subjects, average error variances for identical tests were calculated, along with the mean of the mean errors and the variance of the means. The input-output relations, time delay, amplitude error, and the uncorrelated noise were also averaged over the subjects in a similar manner.

RESULTS

Pursuit Tracking Tasks

For easy comparison, the results of the two types of tracking tasks will be reported in parallel.

As a gross performance measure, the standard deviation was chosen to conform with earlier studies, and the root mean of the total system variances of the errors, σ_p, was calculated to remove the effect of the individual subjects. Summary results of the tests are shown in figures 9 and 10. The data

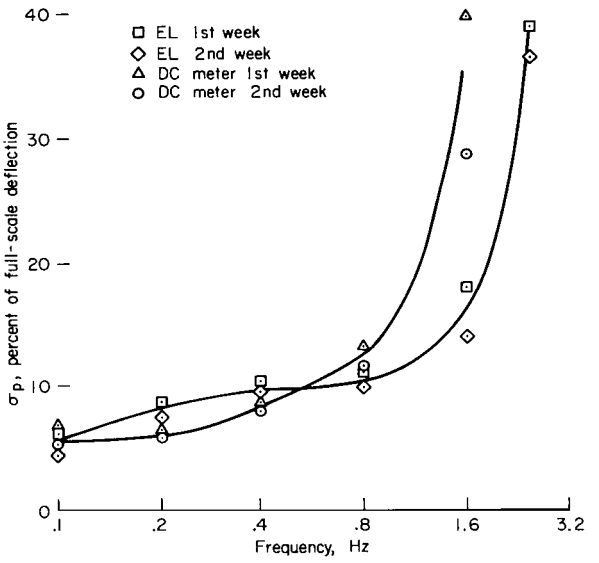

Figure 9.- Error for the sine wave tracking task.

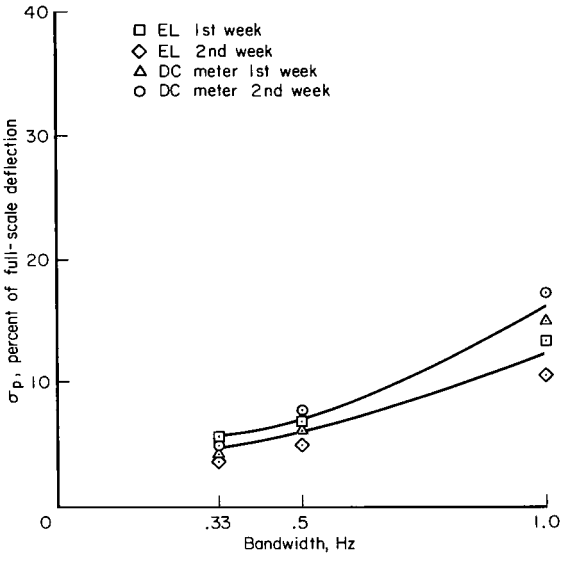

Figure 10.- Error for the random tracking task.

points illustrate that the subjects were sufficiently trained so that there were no significant effects of learning. The measured error was due to the combined characteristics of the man and display. Since the same subjects were used for the two different displays, comparison of the results indicates the merits of the individual instruments alone for the given tasks. The mean of the errors and the variance of the means are not shown. The mean of the errors, however, was found to center around zero, and the variances of the mean error were found to increase as the tracking task became more difficult at higher frequencies or bandwidths.

Figures 9 and 10 show the performance of the instruments for the two tracking tasks. The increase in error above 1.5 Hz with the EL instrument is due to the limited human response capability. In order to better understand the sources of errors, a scoring system was developed for the pursuit tracking task. As shown in appendix B, the tracking output is expressed as $f_f(t) = af_c(t + \tau_d) + \varepsilon_u(t)$, where τ_d is the time delay of the follow-up function, a is the amplitude gain factor, and $\varepsilon_u(t)$ the remnant or

uncorrelated error. Figures 11 to 16 are summary curves of the time delay, τ_d, the amplitude error (1 - a), and the standard deviation of the uncorrelated error.

Time delay, τ_d, was calculated by determining the time shift required for maximum cross correlation between command and follow-up signals. In general, the combined man-instrument time delay between command and follow-up functions becomes larger for instruments with smaller bandwidths. For the sine wave tracking tasks, the input-output time delays shown in figure 11 are relatively small since the subjects could provide sufficient lead to overcome the systems lags. For the EL instrument, the human actually provided a larger lead than was necessary. For the random wave tracking task (fig. 12) the time delay is always positive, since the subject does not know what the command signal will be. The slower instrument response resulted in longer time delays. Errors due to time delay comprise a large part of the total root mean square error discussed previously.

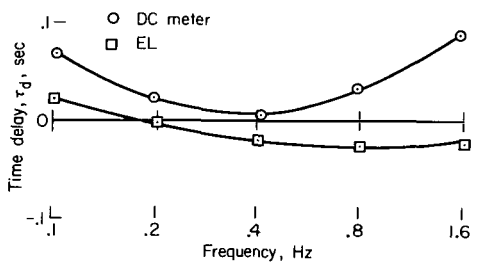

Figure 11.- Time delay for the sine wave tracking task.

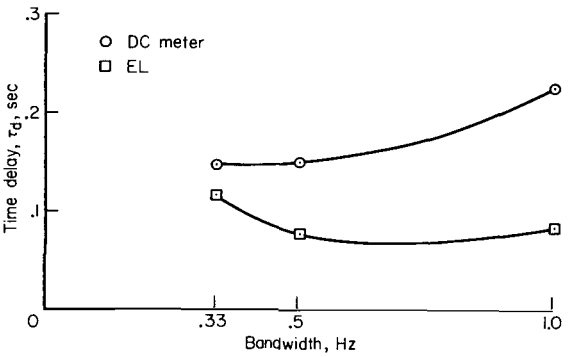

Figure 12.- Time delay for the random wave tracking task.

A further source of error is amplitude error (figs. 13 and 14). As the displayed function moves faster and faster, the human tends to reduce his amplitude response in order to keep up with the motion of the command function. The amplitude is relatively well matched for frequencies up to 1.6 Hz for the EL display and the DC display.

The root mean of the uncorrelated error variances is shown in figures 15 and 16. It is felt that this uncorrelated noise is due to the subject's inability to provide smooth movements.

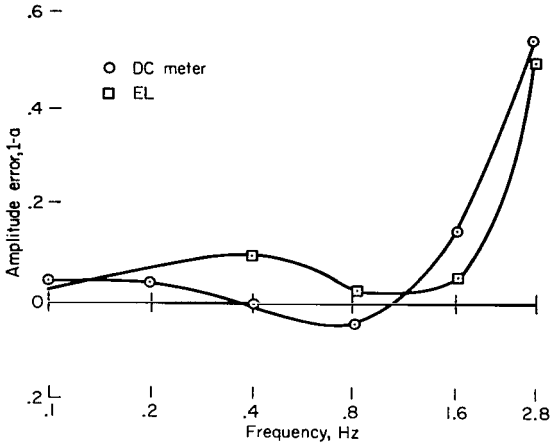

Figure 13.- Amplitude error for the sine wave tracking task.

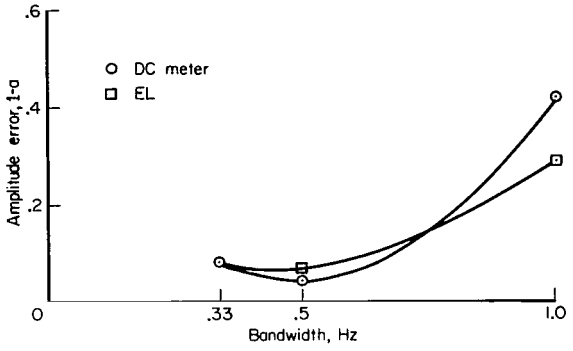

Figure 14.- Amplitude error for the random wave tracking task.

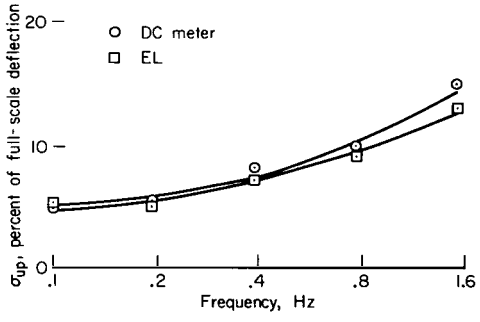

Figure 15.- Uncorrelated noise for the sine wave tracking task.

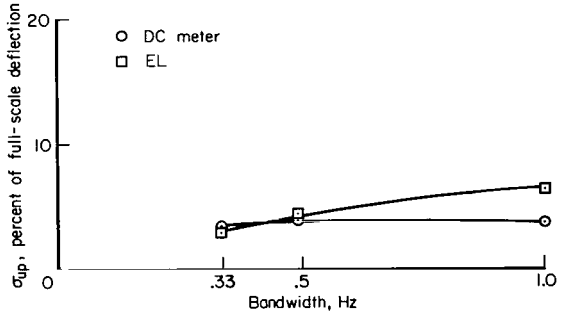

Figure 16.- Uncorrelated noise for the random wave tracking task.

DISPLAY READABILITY TESTS

The results of the reading tests (fig. 17) indicate that the readability of the electroluminescent instruments deteriorates rapidly with increasing environmental illuminance above 550 lm/m^2. However, at the low ambient light conditions expected in a spacecraft environment, less than 1 lm/m^2, the readability is quite adequate. For comparison, when the sun is at zenith, the illumination at the earth's surface is 1100 lm/m^2. The DC meter instrument is less influenced by illumination because the display is brighter. (The brightness of the DC meter is 100 ft-L and the brightness of the EL instrument is 13 ft-L.)

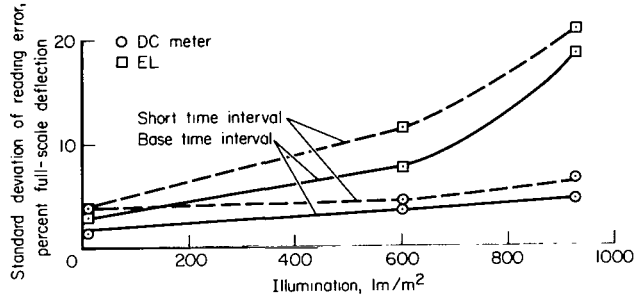

(a) RMS standard deviation for the reading tests.

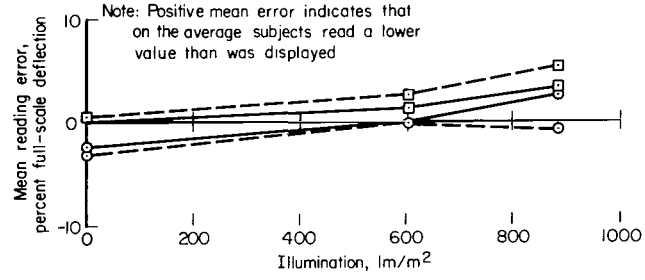

(b) Mean reading error.

Figure 17.- Results of the reading tests.

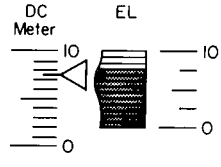

Figure 18.- Instrument scales with indicators: actual size.

The scale resolution of each instrument, as shown in figure 18, illustrates why the DC instrument has a slightly better readability at comfortable environmental lighting (6 lm/m^2); this, together with the fact that the readability of the DC display does not significantly decrease, indicates that the decrease in readability of the EL display with increasing illuminance is due to its low brightness.

CONCLUSIONS

Several conclusions can be drawn from the results of the investigation.

1. The electroluminescent displays are comparable to the electromechanical displays in tracking tasks in the pass band of both instruments and, predictably, are somewhat better for higher frequency signals, which are attenuated by the DC instrument.

2. Proper low environmental lighting conditions are of great importance for the readability of the electroluminescent instrument. The readability of the EL instrument is not impaired under comfortable environmental light conditions, and would be quite satisfactory for spacecraft use when not used under the illuminance of direct sunlight.

3. The discrete vertical scale of the EL instrument did not appear to cause any problems in either a discrete (reading) task or a continuous (pursuit tracking) task.

Ames Research Center
National Aeronautics and Space Administration
Moffett Field, Calif., 94035, July 1, 1968
125-17-04-01-00-21

REFERENCES

1. Pelligrino, James A.; and Rosenbaum, J. L.: Computer Driven Electroluminescent Vertical Scale Indicator. NASA CR-919, 1967.

2. Pew, R. W.; Duffendack, T. C.; and Fensch, L. K.: Summary of Sine-Wave Tracking Studies. NASA SP-128, 1966, pp. 15-24.

APPENDIX A

GENERATION OF NARROWBAND GAUSSIAN NOISE WITH A FLAT FREQUENCY SPECTRUM

To generate narrowband gaussian noise, wideband gaussian noise was first generated, then digitally filtered. For a good approximation of independent samples of wideband gaussian noise with zero mean, 10 samples from a random number generator with range -1 to +1 were added for each sample. The noise was then digitally filtered to a bandwidth of 1 Hz for an assumed 100 samples per second. The filtering is accomplished as follows. Filtering in the frequency domain

$$G(f) = F(f)H(f) \quad \xrightarrow{f(f)} \boxed{H(f)} \xrightarrow{G(f)} \tag{A1}$$

corresponds to convolution in the time domain

$$g(t) = f(t) * h(t) \quad \xrightarrow{f(t)} \boxed{h(t)} \xrightarrow{g(t)}$$

where

$$h(t) = \mathcal{F}^{-1}[H(f)] \tag{A2}$$

where $\mathcal{F}^{-1}$ is the inverse Fourier transform. For the rectangular filter with a bandwidth of w Hz

$$h(t) = 2W \operatorname{sinc}(2Wt)$$

reduced for $w = 1$ Hz

$$h(t) = \frac{\sin(2\pi t)}{\pi t} \tag{A3}$$

for samples spaced 1/100 second apart,

$$h_n = \frac{\sin(2\pi n/100)}{\pi n/100} \tag{A4}$$

remembering $f(t)$ is a set of samples of wideband Gaussian noise, from (A2) the narrowband Gaussian noise is

$$g_m = \sum_{n=-n_1}^{n_1} f_{m-n} \sin(2\pi n/100)/(\pi n/100)$$

$$= \sum_{n=o}^{n_1} (f_{m-n} + f_{m+n}) \sin(2\pi n/100)/(\pi n/100) \qquad \text{(A5)}$$

Theoretically, $n_1 = \infty$, in practice, however, n = 500 was chosen. Consequently correlation between samples exists only over ±5 seconds. Even though the 500 values of the filter function need to be calculated only once, digital filtering is quite slow, each point requiring 500 multiplications.

In the above manner, a sequence of 500,000 Gaussian noise samples of 1 Hz bandwidth was calculated.

APPENDIX B

DEVELOPMENT OF A SCORING SYSTEM

A few samples of detailed tracking behavior for the random wave tracking task are shown in figure 19. For both instruments, the tracking behavior is shown when the tracking function $f_c(t)$ is presented at different speeds. The dotted reference lines help to show a relative increase in time shift lag of $f_f(t)$ as the signal bandwidth increases. Also the amplitude tends to decrease with increased signal bandwidth. This suggests the following calculations. If the tracking output lags behind the command function by a time τ_d, then

$$f_f(t) = f_c(t + \tau_d)$$

where f_c is the command function applied to the display and f_f the output from the human tracker (τ_d is positive for a lagging output). In addition, f_f may also be of different amplitude from f_c and a random noise may be superimposed on the delayed tracking function. Then

$$f_f(t) = af_c(t + \tau_d) + \varepsilon_u(t) \tag{B1}$$

where $\varepsilon_u(t)$ is the uncorrelated noise, called remnant, and a is the amplitude gain factor. Let us calculate the parameters of (B1) (a and τ_d). To do this we first calculate the crosscorrelation between f_c and f_f

$$\lim_{T\to\infty} \frac{1}{T} \int_{-T/2}^{T/2} f_c(t + \tau) f_f(t) dt$$

$$= \lim_{T\to\infty} \frac{1}{T} \int_{-T/2}^{T/2} f_c(t + \tau)[af_c(t + \tau_d) + \varepsilon_u(t)]dt \tag{B2}$$

using equation (B1)

$$= a \lim_{T\to\infty} \frac{1}{T} \int_{-T/2}^{T/2} f_c(t + \tau) f_c(t + \tau_d) dt + \lim_{T\to\infty} \frac{1}{T} \int_{-T/2}^{T/2} f_c(t + \tau) \varepsilon_u(t) dt$$

the second integral on the right side of equation (B2) will be zero, since f_c and ε_u are uncorrelated. The first integral is essentially an autocorrelation function, which will be a maximum at $\tau = \tau_d$. Hence (B2) can be rewritten as

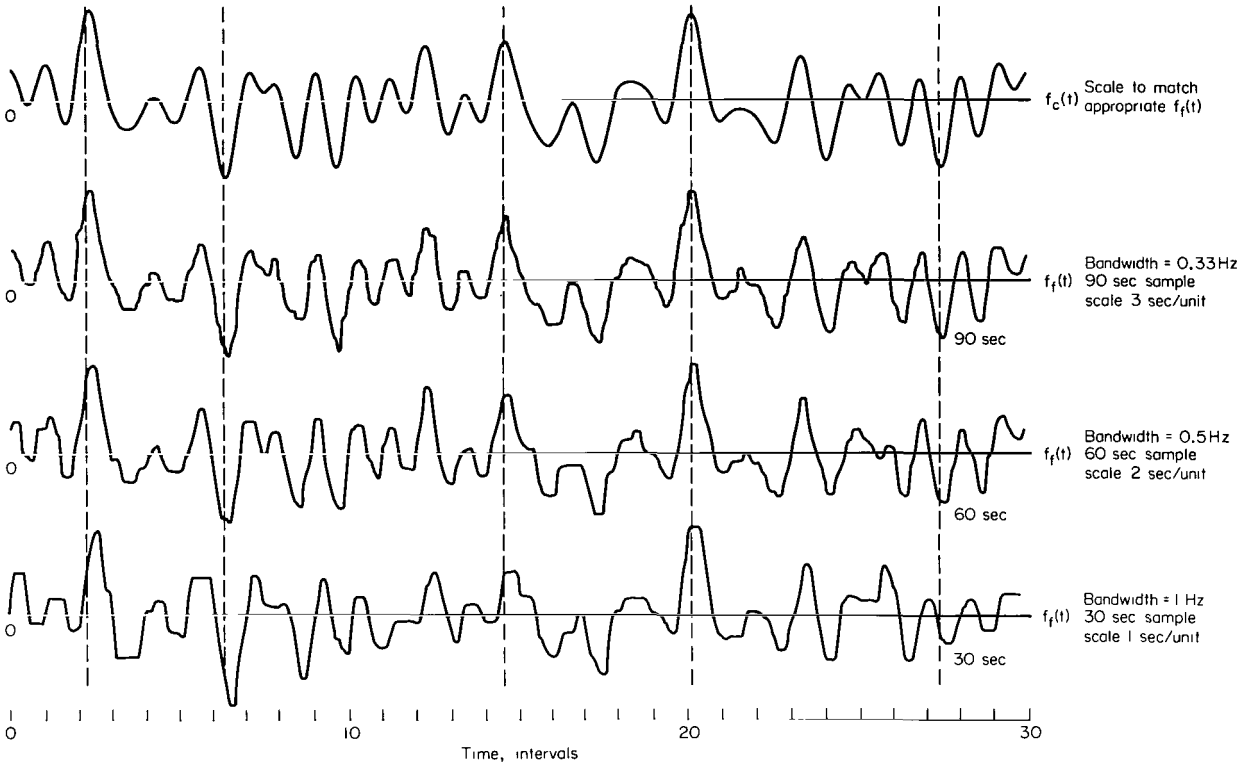

(a) EL instrument.

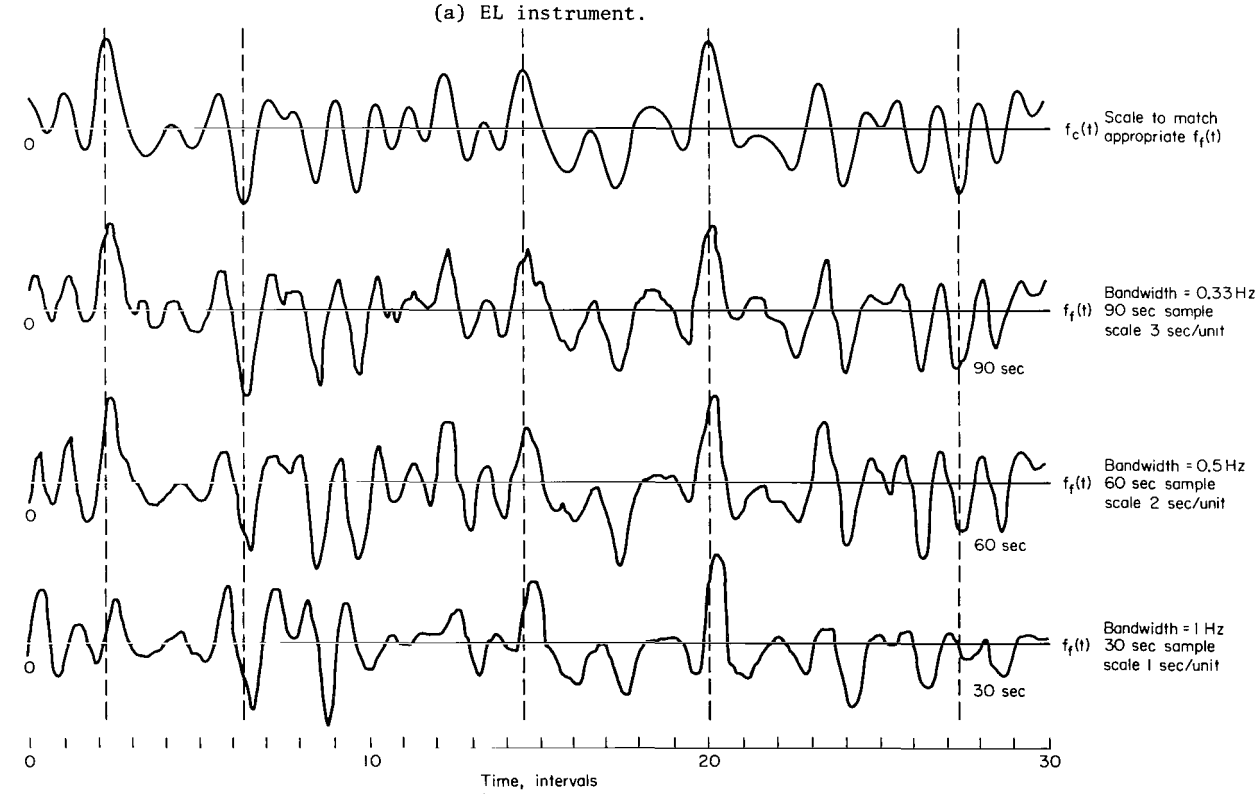

(b) DC instrument.

Figure 19.- Time history of command signal and follow-up signal.

$$\max \lim_{T\to\infty} \frac{1}{T} \int_{-T/2}^{T/2} f_c(t + \tau) f_f(t)dt = a \lim_{T\to\infty} \frac{1}{T} \int_{-T/2}^{T/2} [f_c(t)]^2 dt \qquad \text{(B3)}$$

and

$$a = \frac{\max \lim_{T\to\infty} \int_{-T/2}^{T/2} f_c(t + \tau) f_f(t)dt}{\lim_{T\to\infty} \int_{-T/2}^{T/2} [f_c(t)]^2 dt}$$

is found by determining the value of τ which causes the crosscorrelation expression to be a maximum. The above equations were converted to equivalent summation equations in the same manner as described in appendix A. With the above two parameters, $\varepsilon_u(t)$ can be calculated from equation (B1). Then the variance of the uncorrelated error is

$$\sigma_{u_p}^2 = \sum[\varepsilon_u(t) - \overline{\varepsilon_u(t)}]^2/(n - 1) \qquad \text{(B4)}$$

undoubtedly modeling techniques as used in human performance studies would succeed in describing the input-output relations more accurately, thus resulting in a smaller uncorrelated error.

NASA-Langley, 1968 — 21 A-2898

NATIONAL AERONAUTICS AND SPACE ADMINISTRATION
WASHINGTON, D. C. 20546

OFFICIAL BUSINESS

FIRST CLASS MAIL

POSTAGE AND FEES PAID
NATIONAL AERONAUTICS AND
SPACE ADMINISTRATION

"The aeronautical and space activities of the United States shall be conducted so as to contribute . . . to the expansion of human knowledge of phenomena in the atmosphere and space. The Administration shall provide for the widest practicable and appropriate dissemination of information concerning its activities and the results thereof."

—NATIONAL AERONAUTICS AND SPACE ACT OF 1958

NASA SCIENTIFIC AND TECHNICAL PUBLICATIONS

TECHNICAL REPORTS: Scientific and technical information considered important, complete, and a lasting contribution to existing knowledge.

TECHNICAL NOTES: Information less broad in scope but nevertheless of importance as a contribution to existing knowledge.

TECHNICAL MEMORANDUMS: Information receiving limited distribution because of preliminary data, security classification, or other reasons.

CONTRACTOR REPORTS: Scientific and technical information generated under a NASA contract or grant and considered an important contribution to existing knowledge.

TECHNICAL TRANSLATIONS: Information published in a foreign language considered to merit NASA distribution in English.

SPECIAL PUBLICATIONS: Information derived from or of value to NASA activities. Publications include conference proceedings, monographs, data compilations, handbooks, sourcebooks, and special bibliographies.

TECHNOLOGY UTILIZATION PUBLICATIONS: Information on technology used by NASA that may be of particular interest in commercial and other non-aerospace applications. Publications include Tech Briefs, Technology Utilization Reports and Notes, and Technology Surveys.

Details on the availability of these publications may be obtained from:

SCIENTIFIC AND TECHNICAL INFORMATION DIVISION

NATIONAL AERONAUTICS AND SPACE ADMINISTRATION

Washington, D.C. 20546